Nanoparticle hybrids as efficient theranostic nanoagents with enhanced near-infrared optical absorption and scattering

Qin Chen, Yatao Ren, Hong Qi, et al.

View Online   Export Citation   CrossMark

AIP Advances

Energy Collection

READ NOW!

Nanoparticle hybrids as efficient theranostic nanoagents with enhanced near-infrared optical absorption and scattering

View Online   Export Citation   CrossMark

Qin Chen,[1] Yatao Ren,[1,2] Hong Qi,[2] and Yuying Yan[1,a] (ID)

AFFILIATIONS

[1] Faculty of Engineering, University of Nottingham, Nottingham NG7 2RD, United Kingdom
[2] School of Energy Science and Engineering, Harbin Institute of Technology, Harbin 150001, People's Republic of China

[a] Author to whom correspondence should be addressed: yuying.yan@nottingham.ac.uk

ABSTRACT

The design of high-efficiency theranostic nanoagents that can be utilized in tumor diagnosis and treatment has been investigated extensively in recent years. However, most of the existing nanoagents consist of uncommon materials and complex shell structures. Despite the efforts that have been made, the development of a simple and easily synthesized theranostic nanoplatform that can be applied in optical-based imaging-guided photothermal therapy still remains a challenge. In this paper, we investigated the optical characteristics of nanoparticle aggregates as potential theranostic nanoplatforms. The mechanism of spectrum shifting and the optical properties of contacting and non-contacting short nanochains were investigated. It was found that the near-field interaction of the gold nanosphere will not shift the localized surface plasmon resonance peak to the near-infrared region. However, when the nanospheres are connected to each other, a low energy resonance peak will be excited. On this basis, a simple hybrid theranostic nanoagent consisting of different nanosphere clusters was proposed. The nanohybrid exhibits high absorption and low scattering in the first near-infrared window (NIR-I) and high scattering and near-zero absorption in the second NIR (NIR-II). This characteristic can be beneficial to tumor diagnosis and treatment, i.e., NIR-I for photothermal therapy and NIR-II for optical imaging. Numerical results show that the performance of the proposed hybrid theranostic nanoagent remains excellent even with the existence of potential impurities.

I. INTRODUCTION

Laser-induced thermal therapy (LITT) is emerging as a promising alternative treatment for the early-stage tumor in recent years owing to the absence of side effects.[1–6] During LITT, imaging methods, such as computed tomography (CT),[7] optical imaging,[8,9] and photoacoustic imaging,[10,11] are always applied to provide guidance, such as identifying the location and size of the tumor or monitoring the temperature in the tumorous zone during therapy.[12] As a powerful targeted contrast agent (thermal and optical), plasmonic nanoparticles have been frequently used to enhance the absorption and/or scattering of the tumorous tissue and therefore to initiate hyperthermia of the tumor and hopefully to improve the imaging resolution. To achieve this goal, nanoparticles with different morphologies, sizes, and components have been investigated.

However, until now, not one kind of nanoparticle can be claimed to have the most superior properties to others. This field still remains challenging and needs further investigation. Generally, smaller nanoparticles (diameter smaller than 20 nm) have higher mobility and cellular uptake rate (except phagocytes[13]) compared to their larger counterparts.[14] However, the absorption or scattering ability of smaller nanoparticles in the near-infrared region (optical window) is relatively poor.[15,16] Their absorption and scattering peaks are typically located in the visible region, which is unsuitable for therapy or imaging due to its low penetration depth. Therefore, further investigations are needed to improve the performance of the nanoagents.

Numerous research studies have been reported concerning nanoparticles as theranostic agents in cancer diagnosis and treatment, in which nanoparticles or nanoplatforms are served as

thermal and imaging contrast/enhancing agents. Nanoshell is one of the most popular nanoplatforms under investigation, which allows different shells to have different functions, such as metal or carbon-coated upconversion nanophosphors,[17,18] metal shell dielectric nanoparticles,[19] and polymeride-coated metal nanoparticles.[20] For instance, NaLuF$_4$:Yb,Er@NaLuF$_4$@Carbon was applied to realize high spatial resolution photothermal ablation of labeled tumor *in vivo*, where carbon shell generates heat when interacting with 730-nm laser and NaLuF$_4$:Yb,Er core emitting luminescence under 980-nm excitation, which can be employed to label the tumor (fluorescence imaging) and identify local temperature.[17] Similarly, nanohybrids, which are the mixture of two or more different nanomaterials, also exhibit excellent potential to serve as theranostic agents.[20,21] Except for the above-mentioned theranostic agents, other materials like nanodots[22–24] and nanocapsules[25] are also widely investigated.

Recently, a very promising technique was proposed to improve the localized thermal and optical effect of nanoparticles by using nanochains or other aggregates as contrast agents instead of isolated nanoparticles.[26–29] Specifically, triggered aggregation of gold nanoparticles (GNPs) by legumain is used as contrast agents during chemotherapeutics of brain tumors.[29] It was found that it can enhance the retention of nanoparticles in targeted areas due to the blocking of nanoparticle exocytosis and minimizing nanoparticle backflow to the bloodstream, which is also stimulating for its application in photothermal therapy of other tumors. Thermal triggered assembly of gold nanoparticles is reported to be applied in tumor photothermal therapy and multimodal imaging,[27,28] in which short nanochains of GNPs are observed to enhance the near-infrared light absorption. Thermally triggered assembly of nanoparticles with enhanced optical properties may lead to new directions for the studies of advanced nanoagents for various applications in biomedicine. It should be noted that the absorption peak of gold nanorods can be tuned to the near-infrared region. However, the uptake of nanorods is much smaller than that of nanosphere.[30] Therefore, it is better to use gold nanosphere as theranostic nanoagent if possible. In addition, the above-mentioned short nanochains are formed *in vivo*, which means cellular uptake is not a problem. It should also be noted that luminescence of gold nanoparticles can also be applied for the visualization of biological cells, such as two-photon or multiphoton luminescence, which has also been investigated extensively.[31,32] In this paper, we mainly focus on the light scattering-based optical imaging methods.

Despite the recent success in trying to utilize nanoparticle assemblies in tumor therapy and imaging, the detailed mechanisms for the enhancement of absorption and scattering and the shift of resonance peak from visible to near-infrared still remain unclear. Furthermore, most research studies focus on the absorption properties of nanoparticle assemblies. The scattering properties are always overlooked, which are extremely important for optical-based imaging.[33–37] In this paper, we investigated the near-field interaction between short nanoparticle chains to illustrate the mechanism of the redshift of resonance peak in order to guide the optimization of nanoparticle assemblies in the application of tumor therapy and imaging. Moreover, a simple hybrid theranostic nanoagent was proposed, which exhibits high absorbing and low scattering in the first near-infrared window (NIR-I, from 750 to 900 nm[38]), but high scattering and near-zero absorbing in the second near-infrared

window (NIR-II, from 1000 to 1400 nm[38]). Due to the importance of light–particle interaction and its wide application, several methods have been developed to calculate the optical properties of particles, including Generalized Multiparticle Mie-solution (GMM) Discrete Dipole Approximation (DDA), T-matrix method, Finite Difference Time Domain (FDTD), and Boundary Element Method (BEM). They all have different advantages and disadvantages. In particular, the mesh- or dipole-based methods, such as DDA, FDTD, BEM, or Comsol, are more versatile and suitable for arbitrary-shaped particles. However, they are relatively time-consuming. The GMM and T-matrix methods, which are based on the theoretical solution of Maxwell's equations, have certain limitations but are more efficient. In this paper, short nanochains of spherical particles are applied, where GMM and T-matrix methods are applicable. Therefore, the GMM is adopted.

II. METHODS

Pellegrini *et al.* developed a GMM code to calculate the optical properties of nanoparticle clusters, which are especially suitable for strongly interacting plasmonic spherical particles.[39] For the scattering problem of N-particle cluster, the scattered field of the jth particle can be expressed as[40]

$$\mathbf{E}_{\text{sca},j} = \sum_{n=1}^{\infty} \sum_{m=-n}^{n} i\mathbf{E}_{mn}\left[a_{mn}^{j}\mathbf{N}_{mn}^{(3)} + b_{mn}^{j}\mathbf{M}_{mn}^{(3)}\right], \quad (1)$$

$$\mathbf{H}_{\text{sca},j} = -\frac{k}{\omega\mu}\sum_{n=1}^{\infty} \sum_{m=-n}^{n} \mathbf{E}_{mn}\left[b_{mn}^{j}\mathbf{N}_{mn}^{(3)} + a_{mn}^{j}\mathbf{M}_{mn}^{(3)}\right], \quad (2)$$

where ω is the circular frequency. k is the wavenumber, which satisfies $k^2 = \omega^2\varepsilon\mu$. μ and ε are the permeability and dielectric function of the surrounding medium, respectively. The superscript (3) indicates that the generation function is specified by the Hankel function of the first kind. $\mathbf{E}_{mn}$ is introduced to keep the formulation consistent with that of the Mie theory, which can be expressed as[40]

$$\mathbf{E}_{mn} = |\mathbf{E}_0|i^n(2n+1)\frac{(n-m)!}{(n+m)!}. \quad (3)$$

Then, the interactive scattering coefficients a_{mn}^{j} and b_{mn}^{j} can be obtained by[40]

$$a_{mn}^{j} = a_n^{j}\left\{p_{mn}^{j,j} - \sum_{l\neq j}^{(1,L)}\sum_{v=1}^{\infty}\sum_{\mu=-v}^{v}\left[a_{\mu v}^{l}A_{mn}^{\mu v}(l,j) + b_{\mu v}^{l}B_{mn}^{\mu v}(l,j)\right]\right\}, \quad (4)$$

$$b_{mn}^{j} = b_n^{j}\left\{q_{mn}^{j,j} - \sum_{l\neq j}^{(1,L)}\sum_{v=1}^{\infty}\sum_{\mu=-v}^{v}\left[a_{\mu v}^{l}B_{mn}^{\mu v}(l,j) + b_{\mu v}^{l}A_{mn}^{\mu v}(l,j)\right]\right\}, \quad (5)$$

where L stands for the total sphere number. N is the number of multipolar expansion. a_n^j and b_n^j are the Mie scattering coefficients of the lth sphere. $A_{mn}^{\mu v}(l,j)$ and $B_{mn}^{\mu v}(l,j)$ are the vector translation coefficients.[39] $p_{mn}^{j,j}$ and $q_{mn}^{j,j}$ are the expansion coefficients of the incident wave.

The total scattered field of the particle cluster can be obtained by[40]

$$\mathbf{E}_{sca} = \sum_{n=1}^{\infty} \sum_{m=-n}^{n} i\mathbf{E}_{mn} \left[a_{mn}\mathbf{N}_{mn}^{(3)} + b_{mn}\mathbf{M}_{mn}^{(3)} \right], \quad (6)$$

where a_{mn} and b_{mn} can be expressed as

$$a_{mn} = \sum_{l=1}^{L} \sum_{v=1}^{\infty} \sum_{\mu=-v}^{v} \left[a_{\mu v}^{l} A_{mn}^{\mu v}(l,j_0) + b_{\mu v}^{l} B_{mn}^{\mu v}(l,j_0) \right], \quad (7)$$

$$b_{mn} = \sum_{l=1}^{L} \sum_{v=1}^{\infty} \sum_{\mu=-v}^{v} \left[a_{\mu v}^{l} B_{mn}^{\mu v}(l,j_0) + b_{\mu v}^{l} A_{mn}^{\mu v}(l,j_0) \right]. \quad (8)$$

After the scattered field is determined, the Poynting vector at any location can be obtained. Then, the extinction, scattering, and absorption cross section can be expressed as[40]

$$C_{ext} = \frac{4\pi}{k^2} \sum_{n=1}^{\infty} \sum_{m=-n}^{n} n(n+1)(2n+1) \times \frac{(n-m)!}{(n+m)!} \text{Re}\left(p_{mn}^{0*} a_{mn} + q_{mn}^{0*} b_{mn} \right), \quad (9)$$

$$C_{sca} = \frac{4\pi}{k^2} \sum_{n=1}^{\infty} \sum_{m=-n}^{n} n(n+1)(2n+1) \times \frac{(n-m)!}{(n+m)!} \left(|a_{mn}|^2 + |b_{mn}|^2 \right), \quad (10)$$

$$C_{abs} = C_{ext} - C_{sca}. \quad (11)$$

Then, the absorption and scattering efficiencies of nanoparticles can be calculated by

$$Q_{abs} = \frac{C_{abs}}{n \cdot \pi R^2}, \quad (12)$$

$$Q_{sca} = \frac{C_{sca}}{n \cdot \pi R^2}, \quad (13)$$

where R is the radius of the nanoparticle, and n is the number of particles in a nanoparticle aggregate. For single nanoparticles, n equals 1. The detailed description can be found in Ref. 40 and will not be repeated here. The dielectric constant of gold is obtained from Ref. 41 with cubic spline interpolation for the intermediate data. In this paper, the GMM code developed by Pellegrini *et al.*[39] was utilized to obtain the absorption and scattering properties of gold nanosphere clusters. If not specified, all the results are averaged for the situations where the polarization directions of the electromagnetic field are perpendicular and parallel to the nanochain axis.

III. RESULTS AND DISCUSSIONS

The gap distance and particle numbers in a nanoparticle chain can be controlled precisely by tuning the surface charge density, potential of mean force, or the corona of ligands surrounding the gold nanoparticles.[42–44] Therefore, we first studied the absorption efficiency of different short nanoparticle chains (Fig. 1).

It can be seen that the near-field interaction of non-contacting nanoparticles will not generate an absorption peak in the near-infrared band. The redshift of absorption peak is limited to the visible region with the increasing of nanoparticle number when the interparticle gap is fixed at 5 nm. However, when nanoparticles are attached to each other, an additional absorption peak will generate in the near-infrared region. Moreover, with the increase in particle number, a redshift of the absorption peak will be observed. Furthermore, for nanoparticle chains consisting of nanospheres with a 40 nm radius, the absorption peak can reach NIR-II. It is also
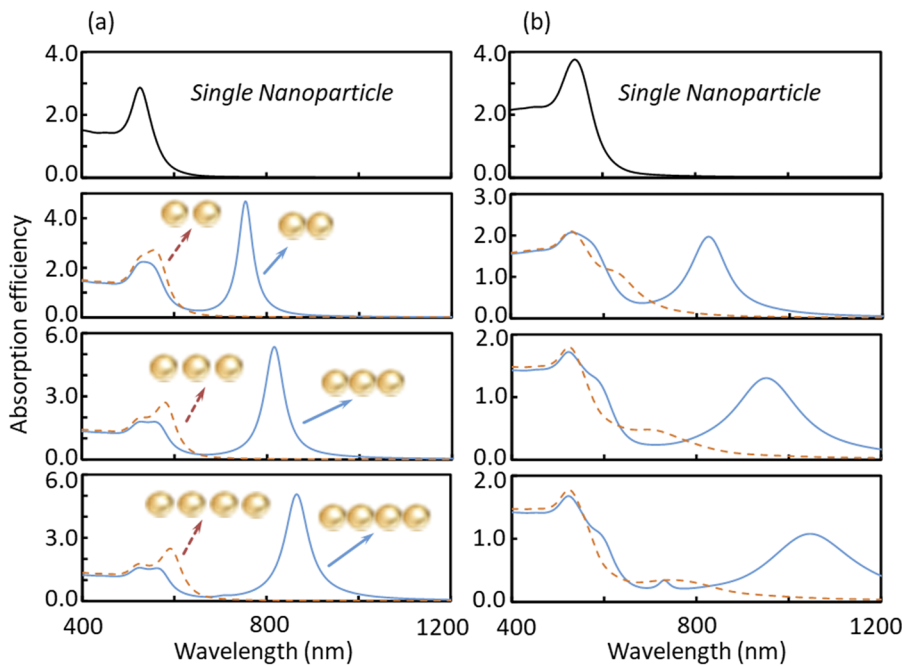
FIG. 1. Absorption efficiency of touching and non-connected (5 nm gap) nanoparticles aggregates (dimer, trimer, and tetramer) consisting of nanoparticles with the same size: (a) R = 20 nm; (b) R = 40 nm.
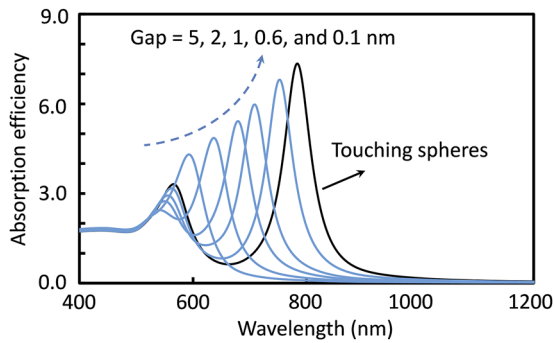
FIG. 2. Absorption efficiency of nanoparticle dimer with different gap distances ($R = 30$ nm for a single nanoparticle).

interesting to note that with increasing of nanoparticle radius and numbers, the resonance linewidth also broadens.

On this basis, we further studied the situations of smaller narrow gaps for nanoparticle dimers (see Fig. 2). For simplicity, the results are only for the situation when the polarization direction of incident light is parallel to the dimer axis. It can be seen that with decreasing of the interparticle gap, the redshift of absorption peak can be observed, which has also been pointed out by Ref. 45. From Figs. 1 and 2, we can know that the additional absorption peak is caused by the redshift due to the interaction of nanoparticles. In the meantime, we should know that even if the nanoparticles in practical applications are not touching with each other, the plasmon resonance can also be tuned to the NIR region with a slight blue shift.

As mentioned, the scattering properties of nanoparticles also need to be investigated to serve as theranostic nanoagent for optical-based imaging-guided photothermal therapy. In general, the potential candidate agent should satisfy the condition that it has a strong absorption and weak scattering in one waveband (for localized heating), and a strong scattering and weak absorption in a separated band (for optical contrast). For small nanoparticles, the absorption and scattering peaks are almost identical with each other, which does not meet the above requirements. For larger nanoparticles, the absorption efficiency is much smaller than the scattering efficiency in the near-infrared range. However, the absorption peak is in the visible region, which is not suitable for thermal therapy due to the strong absorption of biological tissue. Meanwhile, the increase in nanoparticle size will affect the transport of nanoparticles in the human circulatory system (see the supplementary material).

Figure 3 shows the absorption and scattering efficiencies of nanoparticle dimer, trimers, and tetramer with radii of 10, 30, 50, and 80 nm. It can be seen that for the nanochains of smaller nanoparticles ($R = 10$ nm), absorption dominates in the NIR-I region. With the increase in nanoparticle size, the optical properties of nanochains turn from absorption dominated to scattering dominated. In the meantime, the scattering peaks redshift from the NIR-I region to NIR-II region. Most importantly, in the NIR-I region, the scattering efficiencies of larger nanoparticle chains ($R = 80$ nm) are much smaller compared to the absorption efficiencies of smaller nanoparticle chains ($R = 10$ nm). And in NIR-II, the absorption efficiencies of smaller nanoparticle chains are negligible compared to the scattering efficiencies of larger nanoparticle chains. Therefore, it can be realized to use this property of nanoparticles hybrid to optical detection in the NIR-I region and thermal effect in the NIR-II region.
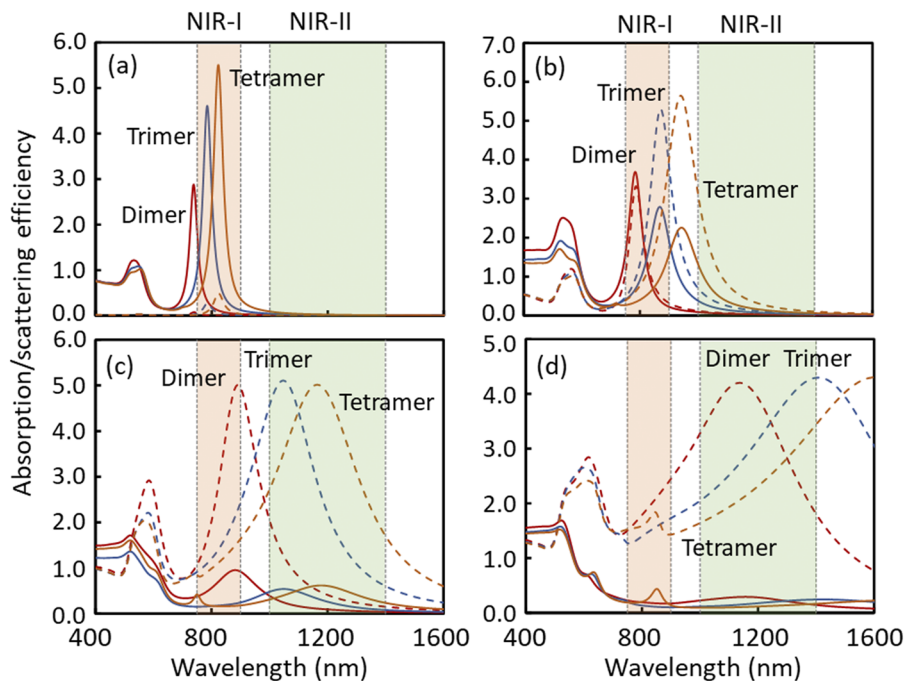
FIG. 3. Absorption and scattering efficiencies of nanoparticle dimer (red lines), trimer (blue lines), and tetramer (orange lines) for different nanoparticle radius: (a) $R = 10$ nm; (b) $R = 30$ nm; (c) $R = 50$ nm; (d) $R = 80$ nm. The solid and dashed lines represent the absorption and scattering efficiencies, respectively.
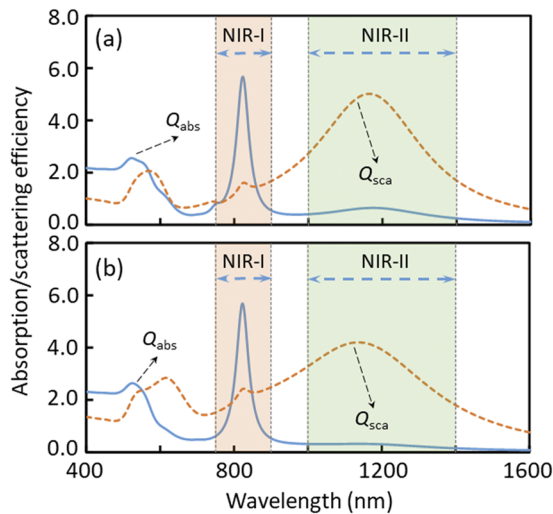
FIG. 4. Absorption and scattering efficiencies of hybrid nanoparticles: (a) Nanosphere tetramer ($R = 10$ nm) + nanosphere tetramer ($R = 50$ nm) and (b) nanosphere tetramer ($R = 10$ nm) + nanosphere dimer ($R = 80$ nm).

To be more specific, here, we show the optical properties of two kinds of nanohybrids (see Fig. 4): one is the hybrid of nanosphere tetramer ($R = 10$ nm) and nanosphere tetramer ($R = 50$ nm), and the other is nanosphere tetramer ($R = 10$ nm) and nanosphere dimer ($R = 80$ nm). It can be seen more clearly that the proposed nanohybrids exhibit high absorbing and low scattering in the NIR-I region and high scattering and near-zero absorbing in the NIR-II region. In addition, it should be noted that in the synthetic or intracellular

FIG. 5. The second absorption peak of the absorption efficiencies and the corresponding ratio of scattering/absorption efficiencies for (a) nanoparticle dimers and (b) nanoparticle tetramers.

triggered process of the nanoparticle chains, there may exist other impurities due to uncontrolled aggregation. For example, in the hybrid shown in Fig. 5(b), there may also exist single nanoparticles ($R = 10$ and 80 nm), dimers ($R = 10$ nm), trimers ($R = 10$ and 80 nm), and tetramers (80 nm). From Figs. 3 and 4, it is obvious that in NIR-I, the absorption ability of the nanoagent is enhanced without improving the scattering ability. Meanwhile, in NIR-II, the scattering ability is enhanced without affecting the absorption efficiency. Therefore, the performance of the proposed theranostic nanoagent is reliable even with potential impurities.

On this basis, the redshift of the second absorption peak of the nanoparticle dimers and tetramers was investigated as a reference for the development of other possible hybrid theranostic nanoagents (see Fig. 5). The absorption and scattering efficiencies were obtained for the situation where the polarization of the incident light is parallel to the nanochain axis. The blue curve shows that with the increase in particle sizes, the absorption/scattering peak has an obvious redshift trend. In the meantime, the nanochains turn from absorption dominating to scattering dominating. Therefore, we can pick from these figures to obtain a nanohybrid that can achieve scattering dominating in the NIR-II region and absorption dominating in the NIR-I region.

IV. CONCLUSIONS

In conclusion, we studied the optical characteristic of short nanoparticle chains (including dimer, trimer, and tetramer). It was found that the near-field interaction between non-contacting nanoparticle short chains will not shift the localized surface plasmon resonance peak to the near-infrared region. However, when the nanospheres are contacted with each other, their absorption and scattering abilities are strongly enhanced in the near-infrared region. Moreover, the scattering and absorption peaks for short nanochain or small nanoparticles are almost identical, which is not suitable for serving as a theranostic nanoagent. However, for larger nanoparticles, the scattering and absorption peaks are apart from each other, with the absorption resonance peak located in the visible region, which is not a good choice for photothermal therapy. Most importantly, it was found that in different near-infrared regions, nanochains of different nanoparticles exhibit different optical properties, to be specific, either scattering dominated or absorption dominated. On this basis, a simple hybrid theranostic nanoagent consisting of different nanoparticle chains without complex shell structures and uncommon materials was proposed. The nanohybrid exhibits high scattering and near-zero absorption in NIR-II, but high absorption and low scattering in NIR-I. This characteristic can be beneficial to the tumor diagnosis and treatment, i.e., NIR-I for photothermal therapy and NIR-II for optical imaging. Numerical results show that the performance of the proposed hybrid theranostic nanoagent remains excellent even with the existence of potential impurities. Future research will be focused on the experimental investigation of the performance of the proposed nanohybrids on optical imaging-guided photothermal therapy.

SUPPLEMENTARY MATERIAL

See the supplementary material for the optical properties of single nanoparticles and the validation of GMM methods.

AUTHOR DECLARATIONS

Conflict of Interest

The authors have no conflicts to disclose.

Author Contributions

Qin Chen: Conceptualization (equal); Investigation (equal); Methodology (equal); Validation (equal); Visualization (equal); Writing – original draft (equal); Writing – review & editing (equal). **Yatao Ren**: Investigation (equal); Methodology (equal); Writing – original draft (supporting); Writing – review & editing (supporting). **Hong Qi**: Conceptualization (equal); Supervision (equal); Writing – review & editing (supporting). **Yuying Yan**: Conceptualization (equal); Funding acquisition (equal); Investigation (equal); Supervision (equal); Writing – review & editing (equal).

DATA AVAILABILITY

The data that support the findings of this study are available from the corresponding author upon reasonable request.

REFERENCES

[1] M. R. Ali, M. A. Rahman, Y. Wu, T. Han, X. Peng, M. A. Mackey, D. Wang, H. J. Shin, Z. G. Chen, H. Xiao, R. Wu, Y. Tang, D. M. Shin, and M. A. El-Sayed, Proc. Natl. Acad. Sci. U. S. A. **114**(15), E3110–E3118 (2017).

[2] N. S. Abadeer and C. J. Murphy, J. Phys. Chem. C **120**(9), 4671–4716 (2016).

[3] G. Chen, I. Roy, C. Yang, and P. N. Prasad, Chem. Rev. **116**(5), 2826–2886 (2016).

[4] M. Sharma, S. Balasubramanian, D. Silva, G. H. Barnett, and A. M. Mohammadi, Expert Rev. Neurother. **16**(2), 223–232 (2016).

[5] Y. Ren, H. Qi, Q. Chen, and L. Ruan, Int. J. Heat Mass Transfer **106**, 212–221 (2017).

[6] Y. Ren, Q. Chen, M. He, X. Zhang, H. Qi, and Y. Yan, ACS Nano **15**(4), 6105–6128 (2021).

[7] Y. Liu, X. Ji, J. Liu, W. W. L. Tong, D. Askhatova, and J. Shi, Adv. Funct. Mater. **27**(39), 1703261 (2017).

[8] M. Cui, S. Liu, B. Song, D. Guo, and Y. He, Nano-Micro Lett. **11**, 73 (2019).

[9] H. Qi, F.-Z. Zhao, Y.-T. Ren, Y.-B. Qiao, L.-Y. Wei, M. A. Islam, and L.-M. Ruan, J. Quant. Spectrosc. Radiat. Transfer **222–223**, 1–11 (2019).

[10] J.-P. Sun, Y.-T. Ren, Z.-X. Liu, M.-J. He, B.-H. Gao, and H. Qi, J. Phys. Chem. C **126**(7), 3489–3501 (2022).

[11] J.-P. Sun, Y.-T. Ren, K. Wei, M.-J. He, B.-H. Gao, and H. Qi, Res. Phys. **34**, 105209 (2022).

[12] J. Wu, D. H. Bremner, S. Niu, M. Shi, and L. Zhu, ACS Appl. Mater. Interfaces **10**(49), 42115–42126 (2018).

[13] S. Behzadi, V. Serpooshan, W. Tao, M. A. Hamaly, M. Y. Alkawareek, E. C. Dreaden, D. Brown, A. M. Alkilany, O. C. Farokhzad, and M. Mahmoudi, Chem. Soc. Rev. **46**(14), 4218–4244 (2017).

[14] N. S. Rosli, A. Abdul Rahman, and A. A. Aziz, Mater. Sci. Forum **756**, 205–211 (2013).

[15] K.-S. Lee and M. A. El-Sayed, J. Phys. Chem. B **109**(43), 20331–20338 (2005).

[16] P. K. Jain, K. S. Lee, I. H. El-Sayed, and M. A. El-Sayed, J. Phys. Chem. B **110**, 7238–7248 (2006).

[17] X. Zhu, W. Feng, J. Chang, Y.-W. Tan, J. Li, M. Chen, Y. Sun, and F. Li, Nat. Commun. **7**, 10437 (2016).

[18] G. Ramírez-García, E. De la Rosa, T. López-Luke, S. S. Panikar, and P. Salas, Dalton Trans. **48**, 9962–9973 (2019).

[19] H. Ke, J. Wang, Z. Dai, Y. Jin, and J. Liu, Angew. Chem., Int. Ed. **50**(13), 3017–3021 (2011).

[20] E. P. Komarala, H. Tyagi, S. Thiyagarajan, L. Pradhan, M. Aslam, and D. Bahadur, J. Mater. Chem. B **5**, 3852–3861 (2017).

[21] N. Kostevšek, I. Abramovič, S. Hudoklin, M. E. Kreft, I. Serša, A. Sepe, J. Vidmar, S. Šturm, M. Spreitzer, and J. Ščančar, Nanoscale **10**, 1308–1321 (2018).

[22] C. Scialabba, A. Sciortino, F. Messina, G. Buscarino, and N. Mauro, ACS Appl. Mater. Interfaces **11**(22), 19854–19866 (2019).

[23] P. Lei, A. Ran, Z. Peng, Y. Shuang, S. Song, L. Dong, X. Xia, K. Du, F. Jing, and H. Zhang, Adv. Funct. Mater. **27**(35), 1702018 (2017).

[24] T. Yang, Y. A. Tang, L. Liu, X. Lv, and H. Chen, ACS Nano **11**(2), 1848–1857 (2017).

[25] H. Ke, J. Wang, S. Tong, Y. Jin, S. Wang, E. Qu, G. Bao, and Z. Dai, Theranostics **4**(1), 12–23 (2014).

[26] C. K. K. Choi, Y. T. E. Chiu, X. Zhuo, Y. Liu, C. Y. Pak, X. Liu, Y.-L. S. Tse, J. Wang, and C. H. J. Choi, ACS Nano **13**(5), 5864–5884 (2019).

[27] S. R. Panikkanvalappil, N. Hooshmand, and M. A. El-Sayed, Bioconjugate Chem. **28**(9), 2452 (2017).

[28] M. Sun, D. Peng, H. Hao, J. Hu, D. Wang, K. Wang, J. Liu, X. Guo, Y. Wei, and W. Gao, ACS Appl. Mater. Interfaces **9**(12), 10453–10460 (2017).

[29] S. Ruan, C. Hu, X. Tang, X. Cun, W. Xiao, K. Shi, Q. He, and H. Gao, ACS Nano **10**(11), 10086–10098 (2016).

[30] B. D. Chithrani, A. A. Ghazani, and W. C. W. Chan, Nano Lett. **6**(4), 662–668 (2006).

[31] J. Olesiak-Banska, M. Waszkielewicz, P. Obstarczyk, and M. Samoc, Chem. Soc. Rev. **48**(15), 4087–4117 (2019).

[32] Q. Ai, H. Zhang, J. Wang, and H. Giessen, ACS Photonics **8**(7), 2088–2094 (2021).

[33] K.-S. Lee and M. A. El-Sayed, J. Phys. Chem. B **110**(39), 19220 (2006).

[34] Y. Wu, M. R. K. Ali, K. Chen, N. Fang, and M. A. El-Sayed, Nano Today **24**, 120–140 (2019).

[35] C. J. Murphy, A. M. Gole, J. W. Stone, P. N. Sisco, A. M. Alkilany, E. C. Goldsmith, and S. C. Baxter, Cheminform **40**(16), 1721–1730 (2009).

[36] Y. Liu, Y. Su, Z. Fan, R. K. Wang, and J. Yao, Proc. SPIE (unpublished) (2004).

[37] F.-Z. Zhao, H. Qi, G. Yao, and Y.-T. Ren, Opt. Express **28**(1), 270–287 (2020).

[38] J.-E. Park, M. Kim, J.-H. Hwang, and J.-M. Nam, Small Methods **1**(3), 1600032 (2017).

[39] G. Pellegrini, G. Mattei, V. Bello, and P. Mazzoldi, Mater. Sci. Eng., C **27**(5–8), 1347–1350 (2007).

[40] Y.-l. Xu, Appl. Opt. **34**(21), 4573–4588 (1995).

[41] P. B. Johnson and R. W. Christy, Phys. Rev. B **6**(12), 4370–4379 (1972).

[42] H. Zhang and D. Wang, Angew. Chem. **47**(21), 3984–3987 (2008).

[43] B. Gao, G. Arya, and A. R. Tao, Nat. Nanotechnol. **7**(7), 433–437 (2012).

[44] G. Wang and R. W. Murray, Nano Lett. **4**(1), 95–101 (2004).

[45] I. Romero, J. Aizpurua, G. W. Bryant, and F. J. García De Abajo, Opt. Express **14**(21), 9988–9999 (2006).